

Analytic Derivation of the Halo Mass Function from the Non-Linear Cosmic Density Field

Laila Linke,^{1*} Johannes Schwinn,¹ Matthias Bartelmann,¹

¹Universität Heidelberg, Institut für Theoretische Astrophysik, Philosophenweg 12, 69120 Heidelberg, Germany

Accepted XXX. Received YYY; in original form ZZZ

ABSTRACT

We estimate the halo mass function (HMF) by applying the excursion set approach to the non-linear cosmic density field. Thereby, we account for the non-Gaussianity of today’s density distribution and constrain the HMF independent of the linear collapse threshold δ_{crit} . We consider a spherical region as a halo, if its density today exceeds the virial overdensity threshold Δ . We model the probability distribution of the non-linear density field by a superposition of a Gaussian and a lognormal distribution, which we constrain with the bispectrum of density fluctuations, predicted by the kinetic field theory description of cosmic structure formation. Two different excursion set approaches are compared. The first treats the density δ as an uncorrelated random walk of the smoothing scale R . The second assumes $\delta(R)$ to be correlated. We find that the resulting HMFs correspond well to the HMF found in numerical simulations if the correlation of $\delta(R)$ is taken into account. Furthermore, the HMF depends only weakly on the choice of the density threshold Δ .

Key words: cosmology: theory – large-scale structure of universe – methods: analytical

1 INTRODUCTION

Explaining the origin and formation of the cosmic large-scale structure is one of the most pressing issues of modern cosmology. An important part of this issue is measuring and explaining the halo mass function (HMF), which describes the number density of dark matter haloes with a given mass and redshift.

The HMF is sensitive to the underlying cosmology and, hence, an important tool to explore the nature of dark matter. One of the main goals of current and future cosmological surveys, such as DES (DES Collaboration et al. 2017), KiDS (de Jong et al. 2017), Euclid (Refregier et al. 2010) or LSST (Ivezic et al. 2008), is the determination of the HMF. A precise and accurate theoretical understanding of the HMF is needed to complement the observational results.

The HMF has been intensely studied in cosmological N -Body simulations, e.g. by Sheth & Tormen (1999), Tinker et al. (2008) and Jenkins et al. (2001). However, these results cannot replace an analytic derivation, which can provide new insights and a better physical understanding.

The first theoretical estimate of the HMF was made by Press & Schechter (1974). Their formalism assumed that the volume fraction filled with haloes of mass $M > M(R)$ is equal to twice the probability of the initial linear density

contrast $\delta(R)$, smoothed on scale R , to be larger than the critical density contrast for spherical collapse $\delta_{\text{crit}} = 1.69$. δ is given in terms of the mean matter density $\bar{\rho}$. This model was refined by Bond et al. (1991), who introduced the excursion set approach. They considered the smoothed initial density field $\delta(R)$ as a random walk with scale R and calculated the probability for a random walk to cross δ_{crit} . Sheth et al. (2001) extended the excursion set approach to account for ellipsoidal collapse.

Even though these approaches compare favourably with the results of cosmological N -Body simulations (see e.g. Sheth & Tormen 1999), they rely on the extrapolation of the linear cosmic density field and assume that a halo is formed at a certain redshift z if the density in the initial density field at z_{ini} is large enough. However, the HMF is a property of the non-linear cosmic density field, as the mean densities in haloes are in the order of $(100 - 300)\bar{\rho}$. Thus, it is preferable to derive the HMF directly from the non-linear cosmic density field. This distribution is strongly non-Gaussian, so higher order statistics, e.g. the bispectrum, are needed to describe it. The deviation from Gaussianity needs to be included in the derivation of the HMF.

In this work, we therefore estimate the HMF from the non-linear cosmic density field. For this, we apply the excursion set approach to the density distribution today. This method estimates the abundance of dark matter haloes by counting spherical regions with an average overdensity above

* E-mail: l.linke@stud.uni-heidelberg.de

a predefined threshold. Therefore, the approach is an analytic analogue to spherical overdensity halo finders, used e.g. by Press & Schechter (1974), Lacey & Cole (1994) or Tinker et al. (2008) in cosmological simulations.

Our approach differs from the conventional derivations of the HMF in three main aspects. First, we account for the non-Gaussianity of today's cosmic density field by estimating the HMF directly from the non-linear density field. Second, since we estimate the HMF from the non-linear density field, we do not need to assume a linear collapse threshold δ_{crit} . Instead, we define a threshold density $\Delta = \frac{\rho_{\text{vir}}}{\bar{\rho}} - 1$ for which we consider an overdensity to be a virialized dark matter halo. However, we find that the HMF depends only weakly on the choice of Δ . Third, in addition to the original excursion set approach by Bond et al. (1991), which assumed the density field δ to be an uncorrelated random walk, we also consider a correlated $\delta(R)$.

To describe the non-Gaussianity of the non-linear cosmic density field, we apply the kinetic field theory description of cosmic structure formation. This theory successfully predicts the non-linear power spectrum of density fluctuations and can also predict the higher order statistics of the cosmic density field. We use the first of those, the bispectrum, to constrain the third cumulant of the density distribution. (c.f. Bartelmann et al. 2016, 2017a,b).

In Section 2, we show how to model the probability density function (PDF) of the non-linear cosmic density field, if its first cumulants are known. We use this modelled PDF in Section 3 to estimate the HMF with excursion sets. For this, we first apply the original excursion set approach by Bond et al. (1991) to the non-linear density field in Subsection 3.1. We then use a modified excursion set approach by Musso & Sheth (2014) in Subsection 3.2 and compare the resulting HMFs with those found in numerical simulations. Section 4 concludes with a summary and a discussion of our findings.

2 MODELLING THE NON-LINEAR DENSITY FIELD

To apply the excursion set approach, a model for the PDF of the cosmic density field is needed. Even though theories of cosmic structure formation provide the higher order statistics of the cosmic density field, the full PDF is not directly obtainable.

A common approach to approximate the PDF from its cumulants is the Edgeworth expansion, as used e.g. by Juszkiewicz et al. (1995). However, this expansion has significant problems, when applied to the non-linear cosmic density field. First, including higher orders of cumulants and more terms does not improve the approximation due to the asymptotic nature of the expansion. Second, there is no clear measure to decide how well the expansion matches the true PDF. Third, the Edgeworth expansion can have negative values and is, therefore, not a proper PDF. A recent evaluation of the use of the Edgeworth expansion for the cosmic density field was conducted by Sellentin et al. (2017).

Instead of applying an Edgeworth expansion, we use a model for the PDF based on two observational and numerical findings. First, the linear density field is well-described by a Gaussian. This is demonstrated by the Gaussianity of the Cosmic Microwave Background (see e.g. Planck Collab-

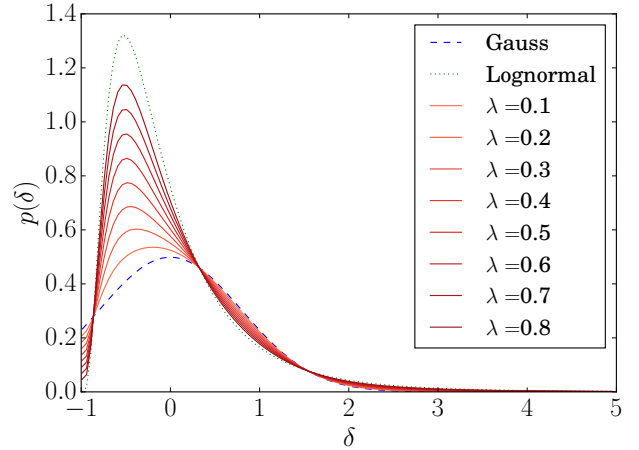


Figure 1. Gauss-lognormal model for different values of λ with fixed $\sigma^2 = 0.5$ (dashed red lines). Also shown: a Gaussian (solid blue line) and a lognormal distribution (solid green line)

oration 2016). Second, the non-linear density field is lognormally distributed, as shown by cosmological N-body simulations, e.g. by Kayo et al. (2001). Consequently, to describe both the linear and the non-linear regime, we adopt the following *Gauss-lognormal model*

$$p(\delta) = (1 - \lambda) \frac{1}{\sqrt{2\pi\sigma^2}} \exp\left[-\frac{(\delta - \mu)^2}{2\sigma^2}\right] + \lambda \frac{1}{\sqrt{2\pi\tilde{\sigma}^2}} \frac{1}{\delta + 1} \exp\left[-\frac{(\ln(\delta + 1) - \tilde{\mu})^2}{2\tilde{\sigma}^2}\right] \quad (1)$$

with

$$\tilde{\mu} = \ln(\mu + 1) - \frac{1}{2} \ln\left(\frac{\sigma^2}{(\mu + 1)^2} + 1\right) \quad (2)$$

$$\tilde{\sigma}^2 = \ln\left(\frac{\sigma^2}{(\mu + 1)^2} + 1\right). \quad (3)$$

This PDF is a linear superposition of a Gaussian and a lognormal distribution, depending on a parameter $\lambda \in [0, 1]$. Both have mean μ and variance σ^2 .

This Gauss-lognormal model is per definition a true PDF because both the Gaussian and the lognormal are normalized and positive on their support. It is fully determined by its first three cumulants: The mean μ is defined to be zero, the variance σ^2 is given by the second cumulant and λ is chosen such that the third cumulant of $p(\delta)$ has a predefined value κ_3 . This results in

$$\lambda = \frac{\kappa_3}{(\sigma^2 + 1)^3 - 3(\sigma^2 + 1) + 2}. \quad (4)$$

Depending on λ this model can describe both the linear and the non-linear cosmic density field. This is demonstrated in Fig. 1. If λ is small, as is the case for a small κ_3 , the PDF is close to a Gaussian, whereas for $\lambda \simeq 1$ it resembles a lognormal distribution. Therefore, the model can be adapted to the linear and the non-linear field with the parameter λ .

We use the expression for κ_3 predicted by the kinetic field theory (c.f. Bartelmann et al. (2016)). In this theory,

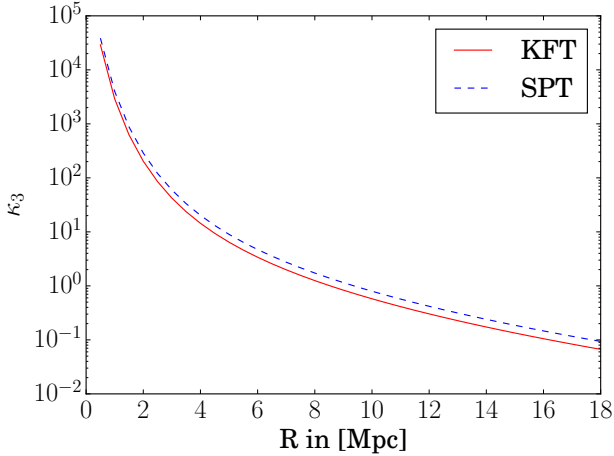


Figure 2. Third cumulant κ_3 of the density distribution as a function of scale R . Both the prediction by the kinetic field theory (solid red) and the standard perturbation theory (dashed blue) are shown.

the bispectrum of the cosmic density field is

$$P^{(3)}(\vec{k}_1, \vec{k}_2, \vec{k}_3) = \delta_D(\vec{k}_1 + \vec{k}_2 + \vec{k}_3) \tau_1^4 \left[P_\delta(k_1) P_\delta(k_2) F(\vec{k}_1, \vec{k}_2) + \text{cyc.} \right] \quad (5)$$

with

$$F(\vec{k}_1, \vec{k}_2) = 1 + \frac{\vec{k}_1 \cdot \vec{k}_2}{k_1^2} + \frac{\vec{k}_1 \cdot \vec{k}_2}{k_2^2} + \frac{(\vec{k}_1 \cdot \vec{k}_2)^2}{k_1^2 k_2^2}.$$

τ_1 is the time-evolution factor and marks at which time the bispectrum is evaluated. It is related to the linear growth function D_+ as:

$$\tau_1 = D_+ - 1 \quad (6)$$

The third cumulant $\kappa_3(R)$ at scale R is

$$\kappa_3 = \int d^3k_1 d^3k_2 d^3k_3 P^{(3)}(\vec{k}_1, \vec{k}_2, \vec{k}_3) \quad (7)$$

$$\begin{aligned} & \hat{W}_R(k_1) \hat{W}_R(k_2) \hat{W}_R(k_3) \\ &= \tau_1^4 \sigma^4 \left(4 + \frac{R}{\sigma^2} \frac{d\sigma^2}{dR} \right). \end{aligned} \quad (8)$$

\hat{W}_R is the Fourier-Transform of the top-hat filter function with radius R .

The third cumulant of the kinetic field theory is similar to that obtained by standard perturbation theory. As shown by [Bernardeau \(1994\)](#), for an Einstein-DeSitter universe $\kappa_{3,\text{SPT}}$ is given as

$$\kappa_{3,\text{SPT}} = \sigma^4 \left(\frac{34}{7} + \frac{R}{\sigma^2} \frac{d\sigma^2}{dR} \right). \quad (9)$$

The closeness between the third cumulant from the kinetic field theory and standard perturbation theory is illustrated in Fig. 2. The prediction for κ_3 by the kinetic field theory remains within 30 per cent of the prediction by standard perturbation theory. We compute the HMF with both the κ_3 by the kinetic field theory and $\kappa_{3,\text{SPT}}$ and compare the results in Section 3.2.

From κ_3 , $\lambda(R)$ can be determined by equation (4). Its

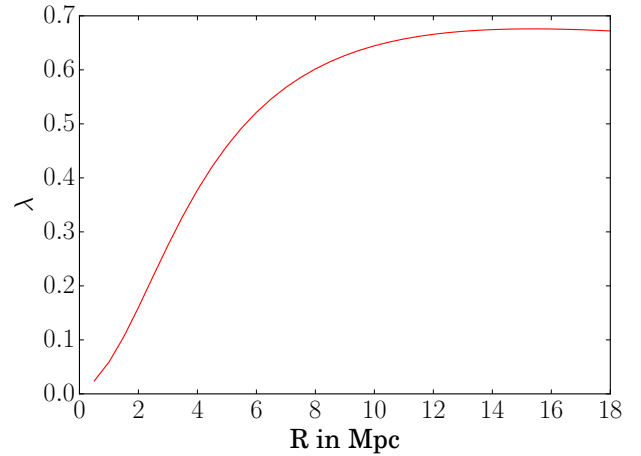


Figure 3. The λ - Parameter of the Gauss-lognormal model for the PDF of the cosmic density field as a function of scale R

evolution with scale is shown in Fig. 3. λ is small for small scales and increases with growing scale. Accordingly, the Gauss-lognormal model approximates the density field by a lognormal at large scales.

With λ , we can obtain the PDFs of the density distribution for different scales, shown in Fig. 4. As expected, the modelled distributions resemble a lognormal at large scales ($R = 10$ Mpc). For small scales ($R = 2$ Mpc), the tails of the distributions reflect the Gaussian. However, the distribution still peaks at low densities, leading to heavily skewed distributions. Therefore, even for small values of λ , the non-Gaussianity of the density field is reflected by the Gauss-lognormal model.

3 APPLYING THE EXCURSION SET APPROACH TO THE NON-LINEAR DENSITY FIELD

Having defined a model for the PDF of the non-linear density field, we can now apply the excursion set approach ([Bond et al. 1991](#)) to obtain the HMF. In this approach, the evolution of the density δ with the smoothing scale R is modelled by a random walk. The volume fraction $F(R)$ filled with haloes of mass $M > M(R)$ is assumed to be equal to the fraction of random walks, which first cross a density threshold δ_{crit} at scale $\sigma(R)$.

The HMF is then given by

$$n(M)dM = \frac{dF}{dR} \frac{\bar{\rho}}{M} dR. \quad (10)$$

For the computation of the HMF we assume a Λ CDM model with parameters as measured by the Planck satellite ([Planck Collaboration et al. 2016](#)).

The original approach by [Bond et al. \(1991\)](#) modelled $\delta(\sigma)$ by an uncorrelated random walk. However, depending on the choice of filter function by which the density field is smoothed, this assumption becomes incorrect. Instead, $\delta(\sigma)$ is a correlated random walk. Therefore, [Musso & Sheth \(2014\)](#) extended the excursion set approach to account for

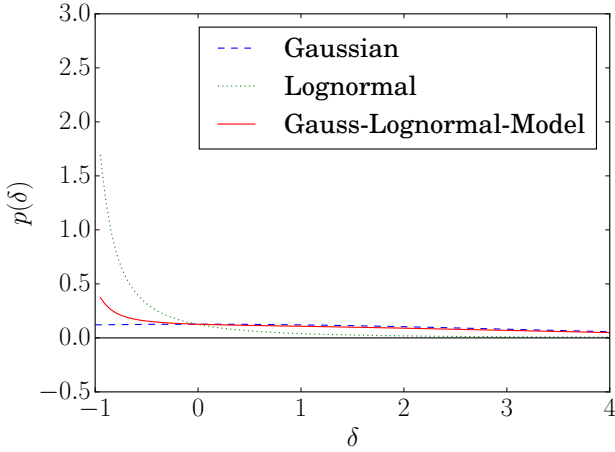
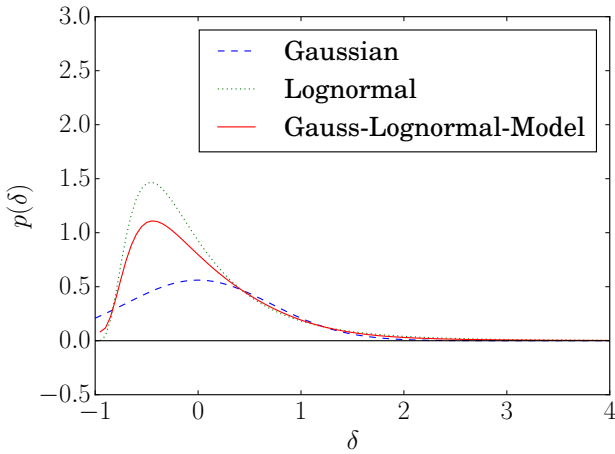
(a) PDF for $R = 2$ Mpc(b) PDF for $R = 10$ Mpc

Figure 4. Probability distribution of the cosmic density contrast δ for the Gauss-lognormal model (solid red), a Gaussian (dashed blue) and a lognormal distribution (dotted green). The top panel (a) shows the PDF for $R = 2$, the bottom panel (b) for $R = 10$.

correlated random walks and applied it to the linear density field.

We apply both the excursion set approaches for uncorrelated and correlated random walks to the non-linear cosmic density field. This requires the choice of a density threshold Δ above which an overdense region is considered collapsed to a halo. This choice is ambiguous. As we are considering the non-linear density field, the linear critical density of spherical collapse ($\delta_{\text{crit}} = 1.69$), used by [Press & Schechter \(1974\)](#), is not applicable. A possible threshold could be the virial overdensity after spherical collapse ($\Delta_{\text{vir}} = 178$). None the less, to remain as unbiased as possible, we leave Δ as a free parameter and calculate the HMF for Δ between 20 and 300. We expect the HMFs with $\Delta \simeq 100 - 200$ to best resemble the HMFs from numerical simulations.

The choice of Δ influences the mass, which is assigned to a halo of a radius R in equation (10), because

$$M = \frac{4\pi}{3} R^3 \bar{\rho}(1 + \Delta). \quad (11)$$

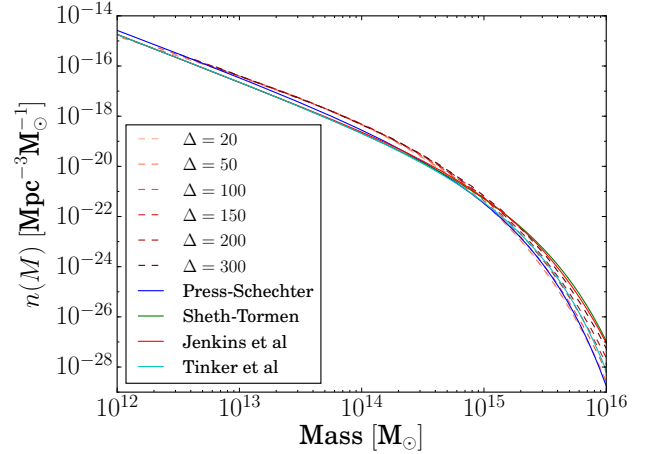


Figure 5. HMF computed from the non-linear density field with the excursion set approach for uncorrelated random walks for different Δ (dashed lines). Also shown: models for the HMF from literature (solid lines)

This mass assignment differs from the usual estimation of the HMF from the linear cosmic density field, as there, the mass is assigned as

$$M_{\text{lin}} = \gamma_f R^3 \bar{\rho}, \quad (12)$$

where γ_f is a constant independent of the choice of density threshold δ_{crit} (c.f. [Lacey & Cole 1994](#)).

3.1 Uncorrelated Random Walk

We first apply the excursion set approach assuming an uncorrelated random walk. In this approach the volume fraction $F(R)$ is given by

$$F(R) = 2 \int_{\Delta}^{\infty} d\delta p(\delta). \quad (13)$$

Inserting our model for the PDF from equation (1) leads to

$$F(R) = 2 \int_{\Delta}^{\infty} d\delta (1 - \lambda) p_G(\delta) + \lambda p_L(\delta + 1). \quad (14)$$

Therefore

$$\begin{aligned} \frac{dF}{dR} = & (1 - \lambda) \frac{\Delta}{\sqrt{2\pi}\sigma^2} \exp\left(-\frac{\Delta^2}{2\sigma^2}\right) \frac{d\sigma}{dR} \\ & + \lambda \frac{1}{\sqrt{\pi}} \exp\left(-\frac{(\ln(\Delta + 1) - \tilde{\mu})^2}{2\tilde{\sigma}^2}\right) \\ & \left[\frac{1}{\sqrt{2}\tilde{\sigma}} \frac{d\tilde{\mu}}{dR} - \frac{\ln(\Delta + 1) - \tilde{\mu}}{\sqrt{2}\tilde{\sigma}} \frac{d\tilde{\sigma}}{dR} \right] \\ & - 2 \frac{d\lambda}{dR} \left[\text{erfc}\left(\frac{\Delta}{\sqrt{2}\sigma}\right) - \text{erfc}\left(\frac{\ln(\Delta + 1) - \tilde{\mu}}{\sqrt{2}\tilde{\sigma}}\right) \right]. \end{aligned} \quad (15)$$

Equation (10) leads then to the HMF.

The resulting HMFs for different Δ are shown in Fig. 5. The choice of Δ does not influence the shape of the HMF for masses lower than $10^{14} M_{\odot}$. At the higher mass tail, however, a larger Δ leads to an increase of the HMF. This increase is due to the relationship between Δ and the halo

masses in equation (11). A higher threshold Δ leads to picking haloes with higher densities. At a fixed radius R , this implies higher halo masses. Therefore, haloes, which would have lower masses for a smaller Δ are now counted as higher mass haloes and the whole mass function is shifted to the right. Consequently, since $n(M)$ is monotonically decreasing, a larger $n(M)$ is assigned to higher mass clusters.

Fig. 5 also shows the HMFs by Press & Schechter (1974), Sheth & Tormen (1999), Tinker et al. (2008) and Jenkins et al. (2001). At high masses, the found HMFs resemble the Jenkins- and the Sheth-Tormen mass function for large values of Δ . The calculated HMFs match the Press-Schechter HMF only for $\Delta = 20$, which is much smaller than the $\Delta_{\text{vir}} = 178$ of the spherical collapse model. This is expected because Press & Schechter (1974) used only the linear cosmic density field to calculate today's HMF and, therefore, underpredicted the number of high mass haloes. Even though we apply the same excursion set approach as Press & Schechter (1974), we account for the non-linearity of the cosmic density field with the Gauss-lognormal model and the known third moment of the cosmic density distribution. Thereby, we include massive haloes which the Press-Schechter HMF does not contain.

The comparison of the calculated HMFs to the Tinker HMF suggests $\Delta \simeq 150$, which is close to the virial overdensity of spherical collapse ($\Delta_{\text{vir}} = 178$). We expect the virial overdensity to be a good estimate of Δ because the spherical collapse model is a first approximation of the true process of halo formation. Furthermore, the Tinker HMF was obtained with a spherical overdensity halo finder, which is a numerical equivalent to our analytical calculation. The good agreement indicates the consistency of the excursion set approach with spherical overdensity halo finders. Thus, the Tinker HMF supports our estimate of the HMF.

Our HMF resembles the Jenkins HMF only for large Δ . The Jenkins HMF was found by a friends-of-friends halo finder in a cosmological N-body simulation. In contrast to the spherical overdensity halo finders, this approach also includes asymmetric haloes and consequently, the Jenkins HMF differs from the Tinker HMF at the high mass end. As our approach resembles the spherical overdensity halo finders, the deviation of our HMF to the Jenkins HMF is expected.

None the less, the comparison between the numerical models and the calculated HMF shows that haloes with masses between 10^{13} and $10^{15} M_{\odot}$ are overpredicted by our results, regardless of the choice of Δ . At $M = 10^{14} M_{\odot}$ the deviation of the HMF with $\Delta = 150$ to the Press-Schechter HMF is 43 per cent.

3.2 Correlated Random Walk

We also apply the excursion set approach for correlated random walks by Musso & Sheth (2014). To simplify the calculation of the volume fraction $F(R)$, they considered all random walks that crossed the threshold Δ in an upward direction and not only those crossing for the first time. This approximation improves with increasing correlation between the steps of the random walk and is most accurate for strongly correlated walks because for these the probability of crossing the threshold twice is low.

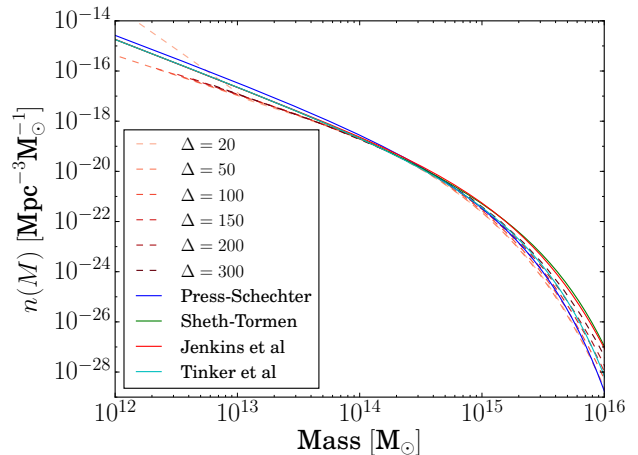


Figure 6. HMF computed from the non-linear density field with the excursion set approach for correlated random walks for different Δ (dashed lines). Also shown: models for the HMF from literature (solid lines)

Consequently, $F(R)$ is

$$F(R) = \int_{-\infty}^{\sigma(R)} d\sigma \int_0^{\infty} d\left(\frac{d\delta}{d\sigma}\right) p\left(\delta, \frac{d\delta}{d\sigma}\right) \frac{d\delta}{d\sigma} \quad (16)$$

$$= \int_{-\infty}^{\sigma(R)} d\sigma \int_0^{\infty} d\delta' p(\delta, \delta') \delta' \frac{dR}{d\sigma}. \quad (17)$$

where $p(\delta, \delta')$ is the joint PDF of the density δ and its derivative $\delta' = \frac{d\delta}{dR}$. We use the Gauss-lognormal model for the PDF of the density distribution, which leads to the joint PDF

$$p(\delta, \delta') = \frac{1 - \lambda}{2\pi|C|^{1/2}} \exp\left[-\frac{1}{2|C|} \left(\delta^2 \frac{d^2\sigma^2}{dR^2} - 2\delta\delta' \frac{d\sigma^2}{dR} + \delta'\sigma^2\right)\right] + \frac{\lambda}{2\pi|C|^{1/2}(\delta + 1)^2} \exp\left[-\frac{1}{2|C|} \left((\ln(\delta + 1) - \tilde{\mu})^2 \frac{d^2\tilde{\sigma}^2}{dR^2} - 2(\ln(\delta + 1) - \tilde{\mu}) \left(\frac{\delta'}{1 + \delta} - \tilde{\mu}'\right) \frac{d\tilde{\sigma}^2}{dR} + \left(\frac{\delta'}{1 + \delta} - \tilde{\mu}'\right)^2 \tilde{\sigma}^2\right)\right]. \quad (18)$$

Equation (17) implies

$$\frac{dF}{dR} = \frac{dF}{d\sigma} \frac{d\sigma}{dR} \quad (19)$$

$$= - \int_{-\infty}^0 d\left(\frac{d\delta}{dR}\right) p\left(\delta, \frac{d\delta}{dR}\right) \frac{d\delta}{dR}. \quad (20)$$

Inserting equations (20) and (18) into equation (10) leads to the HMF. The results for different Δ are shown in Fig. 6. Similar to the HMFs from uncorrelated random walks, Δ has only a weak influence on the shape of the HMF at $M < 10^{14} M_{\odot}$. Larger values of Δ result in an increase of the HMF for larger mass haloes.

In contrast to the HMFs from uncorrelated random

walks, the HMFs shown in Fig. 6 do not overpredict medium sized haloes. Instead, for $M > 5 \cdot 10^{13} M_{\odot}$ the HMFs agree with the numerical models. Therefore, including the correlations of the random walk improves the estimate of the HMF.

However, haloes with masses lower than $5 \cdot 10^{13} M_{\odot}$ are underpredicted compared to the numerical models. This is due to the overcounting of random walks with multiple crossings. The contribution of overcounted random walks has to be subtracted from F in equation (17). Since $\frac{d\sigma}{dR} < 0$, equation (20) implies that the contribution must be added to $\frac{dF}{dR}$ and, consequently, to $n(M)$. Hence, $n(M)$ is too small. The underprediction is stronger at low masses because the probability for multiple crossings is higher for larger σ . Therefore, including multiple crossings can improve the estimated HMFs.

In the high mass regime the HMFs in Fig. 6 based on correlated random walks are almost identical to those based on uncorrelated random walks in Fig. 5. They also agree with the Press-Schechter HMF for the low value $\Delta = 20$ and Tinker HMF for $\Delta = 150$. Thus, the correlations of the random walks are negligible at high masses.

Instead of using the third cumulant κ_3 of the kinetic field theory from equation (7), it is also possible to constrain the PDF of the density field and, hence, the HMF with the third cumulant $\kappa_{3,\text{SPT}}$ from standard perturbation theory in equation (9). We now use this third cumulant to compute the HMF for a correlated random walk with equation (20). This allows a comparison of the standard perturbation theory to the kinetic field theory.

The HMF using standard perturbation theory is shown for different Δ in Fig. 7. Comparing this HMF with the one in Fig. 6 shows that with standard perturbation theory a slightly higher number of large mass clusters ($M > 10^{14} M_{\odot}$) are predicted. However, the differences between the results of standard perturbation theory and kinetic field theory are small compared to the deviations between the numerical models for the HMF at high masses, so it is unclear which of the two theories is to be preferred.

4 CONCLUSION

In this work, we derive analytically the halo mass function (HMF) from the non-linear cosmic density field by applying two different excursion set approaches. The first approach is based on Bond et al. (1991) and assumes the density $\delta(R)$ to be a random walk with uncorrelated steps. The second approach is based on Musso & Sheth (2014). It accounts for correlations in the random walk. We model the distribution of the non-linear cosmic density field by a linear superposition of a Gaussian and a lognormal probability distribution, constrained by the first three moments predicted from the kinetic field theory by Bartelmann et al. (2016).

The HMFs from both approaches depend only weakly on the choice of the critical density Δ . Different Δ lead to similar HMFs for small masses and deviations are only visible at the high mass end. The resulting HMFs resemble the Tinker HMF ((Tinker et al. 2008)) for $\Delta = 150$. This is close to $\Delta_{\text{vir}} = 178$, expected from the spherical collapse model, and demonstrates the consistency between our analytical calculation and the numerical determination of the HMF.

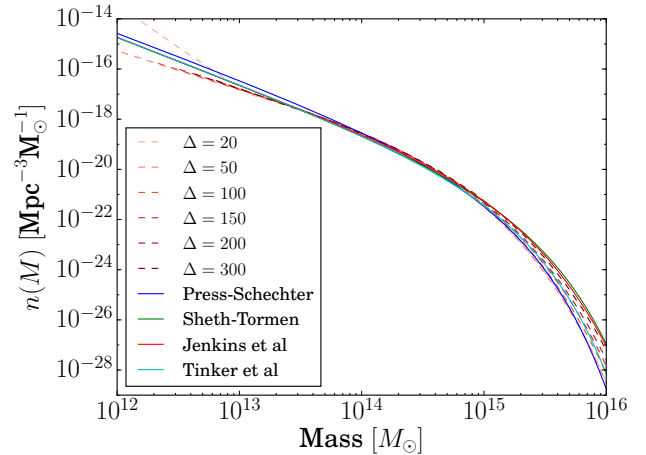


Figure 7. HMF computed from the non-linear density field constrained by standard perturbation theory with the excursion set approach for correlated random walks for different Δ (dashed lines). Also shown: models for the HMF from literature (solid lines)

Comparing the results of both approaches indicates that including the correlation in the random walk should be preferred. At masses between $M = 10^{13}$ and $10^{14} M_{\odot}$, the HMFs based on uncorrelated random walks overestimate the number of haloes. The HMFs based on correlated random walks resemble numerical predictions closer, but slightly underestimate haloes of masses lower than $10^{13} M_{\odot}$. Refining the approach by Musso & Sheth (2014) by considering all correlated random walks would reduce the underestimation.

We also showed that even though the kinetic field theory and the standard perturbation theory for cosmic structure formation originate from fundamentally different assumptions on the cosmic matter field, their predictions for the third cumulant of the cosmic density distribution are close. Therefore, the HMFs resulting from our excursion set approach are similar for both theories of structure formation.

ACKNOWLEDGEMENTS

We would like to thank the ITA cosmology group, especially Sara Konrad and Felix Fabis, as well as Björn Schäfer for many helpful discussions. JS acknowledges financial support from the Heidelberg Graduate School of Fundamental Physics (HGSFP).

REFERENCES

- Bartelmann M., Fabis F., Berg D., Kozlikin E., Lilow R., Viermann C., 2016, *New Journal of Physics*, 18, 043920
- Bartelmann M., Fabis F., Konrad S., Kozlikin E., Lilow R., Littek C., Dombrowski J., 2017a, preprint, ([arXiv:1710.07522](https://arxiv.org/abs/1710.07522))
- Bartelmann M., Fabis F., Kozlikin E., Lilow R., Dombrowski J., Mildenerger J., 2017b, *New Journal of Physics*, 19, 083001
- Bernardeau F., 1994, *ApJ*, 433, 1
- Bond J. R., Cole S., Efstathiou G., Kaiser N., 1991, *ApJ*, 379, 440

- DES Collaboration et al., 2017, preprint, ([arXiv:1708.01530](#))
- Ivezic Z., Tyson J. A., Abel B., Acosta E., for the LSST Collaboration 2008, preprint, ([arXiv:0805.2366](#))
- Jenkins A., Frenk C. S., White S. D. M., Colberg J. M., Cole S., Evrard A. E., Couchman H. M. P., Yoshida N., 2001, *MNRAS*, 321, 372
- Juszkiewicz R., Weinberg D. H., Amsterdamski P., Chodorowski M., Bouchet F., 1995, *ApJ*, 442, 39
- Kayo I., Taruya A., Suto Y., 2001, *ApJ*, 561, 22
- Lacey C., Cole S., 1994, *MNRAS*, 271, 676
- Musso M., Sheth R. K., 2014, *MNRAS*, 439, 3051
- Planck Collaboration 2016, *A&A*, 594, A16
- Planck Collaboration et al., 2016, *A&A*, 594, A13
- Press W. H., Schechter P., 1974, *ApJ*, 187, 425
- Refregier A., Amara A., Kitching T. D., Rassat A., Scaramella R., Weller J., Euclid Imaging Consortium f. t., 2010, preprint, ([arXiv:1001.0061](#))
- Sellentin E., Jaffe A. H., Heavens A. F., 2017, preprint, ([arXiv:1709.03452](#))
- Sheth R. K., Tormen G., 1999, *MNRAS*, 308, 119
- Sheth R. K., Mo H. J., Tormen G., 2001, *MNRAS*, 323, 1
- Tinker J., Kravtsov A. V., Klypin A., Abazajian K., Warren M., Yepes G., Gottlöber S., Holz D. E., 2008, *ApJ*, 688, 709
- de Jong J. T. A., et al., 2017, *A&A*, 604, A134

This paper has been typeset from a $\text{\TeX}/\text{\LaTeX}$ file prepared by the author.